Interferometric Bell-state preparation using femtosecond-pulse-pumped spontaneous parametric down-conversion

Yoon-Ho Kim,* Maria V. Chekhova,† Sergei P. Kulik,† Morton H. Rubin, and Yanhua Shih
Department of Physics, University of Maryland, Baltimore County, Baltimore, Maryland 21250
(Received 6 December 2000; published 7 May 2001)

We present a theoretical and experimental study of preparing maximally entangled two-photon polarization states, or Bell states, using femtosecond-pulse-pumped spontaneous parametric down-conversion (SPDC). First, we show how the inherent distinguishability in femtosecond-pulse-pumped type-II SPDC can be removed by using an interferometric technique without spectral and amplitude postselection. We then analyze the recently introduced Bell-state preparation scheme using type-I SPDC. Theoretically, both methods offer the same results, however, type-I SPDC provides experimentally superior methods of preparing Bell states in femtosecond-pulse-pumped SPDC. Such a pulsed source of highly entangled photon pairs is useful in quantum communications, quantum cryptography, quantum teleportation, etc.

DOI: 10.1103/PhysRevA.63.062301 PACS number(s): 03.67.Hk, 42.50.Dv

I. INTRODUCTION

The nature of quantum entanglement attracted a great deal of attention even in the early days of quantum mechanics, yet it remained an unsolvable subject of philosophy until Bell showed the possibility of practical experimental tests [1–4]. Since then, many experimental tests on the foundations of quantum mechanics have been performed [5–8]. All these tests confirmed quantum-mechanical predictions. More recently, experimental and theoretical efforts are being shifted to ''applications,'' such as quantum communications, quantum cryptography [9], and quantum teleportation [10], taking advantage of the peculiar physical properties of quantum entanglement. It is clear that preparation of maximally entangled two-particle (two-photon) entangled states, or Bell states, is an important subject in modern experimental quantum optics.

By far the most efficient source of obtaining two-particle entanglement is spontaneous parametric down conversion (SPDC). SPDC is a nonlinear optical process in which a higher-energy pump photon is converted into two lower-energy daughter photons, usually called the signal and the idler, inside a noncentrosymmetric crystal [11]. In type-I SPDC, both daughter photons have the same polarizations but in type-II SPDC, the signal and the idler photons have orthogonal polarizations. The signal and the idler are generated into a nonfactorizable entangled state. The photon pair is explicitly correlated in energy and momentum or equivalently in space and time. To prepare a maximally entangled two-photon polarization state, or a Bell state, one has to make appropriate local operations on the SPDC photon pairs.

The polarization Bell states, for photons, can be written as

$$|\Phi^{\pm}\rangle = |X_1, X_2\rangle \pm |Y_1, Y_2\rangle,$$

$$|\Psi^{\pm}\rangle = |X_1, Y_2\rangle \pm |Y_1, X_2\rangle, \quad (1)$$

where the subscripts 1 and 2 refer to two different photons, photon 1 and photon 2, respectively, and they can be arbitrarily far apart from each other. $|X\rangle$ and $|Y\rangle$ form the orthogonal basis for the polarization states of a photon, for example, it can be horizontal ($|H\rangle$) and vertical ($|V\rangle$) polarization state, as well as $|45°\rangle$ and $|-45°\rangle$, respectively.

The subject of this paper is a detailed theoretical and experimental account of how one can prepare a polarization Bell state using femtosecond-pulse-pumped SPDC. In Sec. I, we discuss why one needs such a pulsed source of Bell states, what happens when femtosecond-pulsed laser is used to pump a type-II SPDC, and what has been done to recover the visibility of quantum interference in femtosecond-pulse pumped type-II SPDC. In Sec. II, we present a detailed theoretical description of how one can prepare a polarization Bell state using femtosecond-pulse-pumped type-II SPDC without any postselection, followed by the experiment in Sec. III. We then turn our attention to type-I SPDC and investigate it in detail theoretically in Sec. IV and experimentally in Sec. V.

The quantum nature of SPDC was first studied by Klyshko in late 1960's [12]. Zel'dovich and Klyshko predicted the strong quantum correlation between the photon pairs in SPDC [13], which was first experimentally observed by Burnham and Weinberg [14]. The nonclassical properties of SPDC were first applied to develop an optical brightness standard [15] and absolute measurement of detector quantum efficiency [16].

Shih and Alley first used the quantum interference effect in SPDC for the preparation of a Bell state [7]. Hong, Ou, and Mandel later used it to demonstrate the ''photon bunching'' effect [17]. These experiments have used type-I noncollinear SPDC and a beamsplitter to superpose the signal-idler amplitudes. Experimentally, type-I noncollinear SPDC is not an attractive way of preparing a Bell state mostly due to the difficulties involved in alignment of the system. Collinear type-II SPDC developed by Shih and Sergienko resolved this issue [18]. There is, however, a common problem; the entangled photon pairs have a 50% chance of leaving at the same output ports of the beam splitter. Therefore, the state prepared after the beam splitter may not be

*Email address: yokim@umbc.edu
†Permanent address: Department of Physics, Moscow State University, Moscow, 119899, Russia.

considered as a Bell state without amplitude postselection as pointed out by De Caro and Garuccio [19]. Only when one considers the coincidence contributing terms by throwing away two out of four amplitudes (postselection of 50% of the amplitudes) the state is then considered to be a Bell state. Kwiat *et al* solved this problem by using noncollinear type-II SPDC [20]. This noncollinear type-II SPDC method of preparing a Bell state has been widely used in the quantum optics community.

Recently, cw pumped type-I SPDC has also been used to prepare Bell states. Kwiat *et al.* used two thin nonlinear crystals to prepare Bell states using noncollinear type-I SPDC [21] and Burlakov *et al.* used a beamsplitter to join collinear type-I SPDC from two thick crystals in a Mach-Zehnder interferometer type setup [22].

Therefore, in cw pumped SPDC, there are readily available well-developed methods of preparing a Bell state. However, entangled photon pairs occur randomly within the coherence length of the pump-laser beam. This huge time uncertainty makes it difficult to use in some applications, such as the generation of multiphoton entangled states, quantum teleportation, etc, as interactions between entangled photon pairs generated from different sources are required. This difficulty was thought to be solved by using a femtosecond-pulse laser as a pump. Unfortunately, femtosecond-pulse-pumped type-II SPDC shows poor quantum interference visibility due to the very different (compared to the cw case) behavior of the two-photon effective wave function [23]. One has to utilize special experimental schemes to maximize the overlap of the two-photon amplitudes. Traditionally, the following methods were used to restore the quantum interference visibility in femtosecond-pulse-pumped type-II SPDC: (i) to use a thin nonlinear crystal ($\simeq 100\ \mu$m) [24] or (ii) to use narrow-band spectral filters in front of detectors [25]. Both methods, however, reduce the available flux of the entangled photon pair significantly and cannot achieve complete overlap of the wave functions in principle. We will discuss this in detail in Sec. II.

Branning *et al.* first reported an interferometric technique to remove the intrinsic distinguishability in femtosecond-pulse-pumped type-II SPDC without using narrow-band filters and a thin crystal [26]. This method, however, cannot be used to prepare a Bell state since *four* biphoton amplitudes are involved in the quantum interference process [27]. This issue will be discussed in Sec. II. More recently, Atatüre *et al.* claimed recovery of high-visibility quantum interference in pulse-pumped type-II SPDC from a thick crystal without spectral postselection [28]. Unfortunately, the theory as well as the interpretation of the experimental data presented in their work are shown to be in error [29]. Then it is fair to say that there have been no generally accepted methods of preparing a Bell state from femtosecond-pulse-pumped SPDC without making any postselection, especially the spectral postselection. In the following sections, we will present experimental studies of preparing a Bell state using femtosecond-pulse-pumped SPDC (both type II and type I) together with the theoretical analysis.

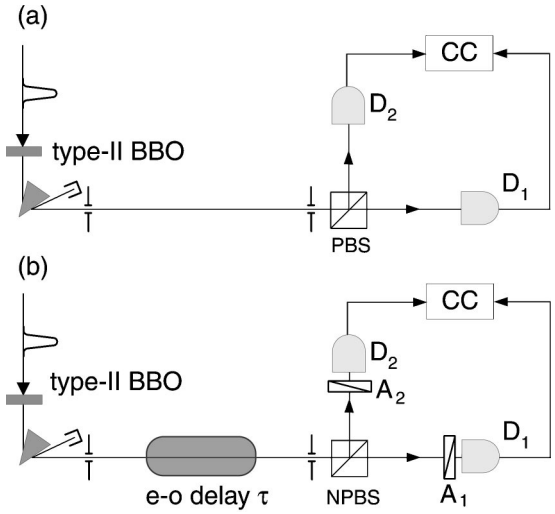

FIG. 1. (a) Most simple two-photon correlation experiment. A femtosecond-pulse pumps a type-II BBO crystal to create entangled photon pairs via the SPDC process. Orthogonally polarized signal and idler photons are separated by a PBS and detected by two detectors D_1 and D_2. (b) Collinear interferometer to observe quantum interference. The *e-o* delay τ can be introduced by a stack of quartz plates. NPBS is a 50/50 nonpolarizing beamsplitter. A_1 and A_2 are polarization analyzers.

II. BELL-STATE PREPARATION USING TYPE-II SPDC: THEORY

Let us first briefly discuss the basic formalism of pulse-pumped type-II SPDC as discussed by Keller and Rubin [23]. A femtosecond-pulse pumps a type-II BBO crystal to create entangled photon pairs via the SPDC process. Orthogonally polarized signal and idler photons are separated by a polarizing beamsplitter (PBS) and detected by two detectors, see Fig. 1(a).

Let us start from the Hamiltonian of the SPDC [23,30]

$$\mathcal{H}=\epsilon_0 \int d^3\vec{r}\chi^{(2)}E_p(z,t)E_o^{(-)}E_e^{(-)}, \tag{2}$$

where $E_p(z,t)$ is the electric field for the pump pulse, which is considered to be classical, and $E_o^{(-)}$ ($E_e^{(-)}$) is the negative frequency part of the quantized electric field for the *o*-polarized (*e*-polarized) photon inside the $\chi^{(2)}$ nonlinear crystal (BBO). The pump field can be written as

$$E_p(z,t)=\mathcal{E}_p \int d\omega_p e^{-[\omega_p-\Omega_p]^2/\sigma_p^2} e^{i[k_p(\omega_p)z-\omega_p t]}, \tag{3}$$

where $\mathcal{E}_p$ is the amplitude of the pump pulse, Ω_p is the central frequency of the pump pulse, $\sigma_p^2=4\ln 2/[\sigma_p^{\mathrm{FWHM}}]^2$ where σ_p^{FWHM} is the full width at half maximum (FWHM) bandwidth of the pump pulse, and the z direction is taken to be the pump pulse propagation direction. In the interaction picture, the state of SPDC is calculated from first-order perturbation theory [30]

$$|\psi\rangle = -\frac{i}{\hbar}\int_{-\infty}^{\infty} dt\, \mathcal{H}|0\rangle,$$

$$= C\int dk_o dk_e d\omega_p \int_o^L dz\, e^{-[\omega_p-\Omega_p]^2/\sigma_p^2} \times e^{i\Delta z}\delta(\omega_o+\omega_e-\omega_p)a_o^\dagger a_e^\dagger|0\rangle, \quad (4)$$

where C is a constant, L is the thickness of the crystal, $a_o^\dagger$ ($a_e^\dagger$) is the creation operator of o-polarized (e-polarized) photon in a given mode, and $\Delta = k_p - k_o - k_e$ is the phase mismatch.

The state vector $|\psi\rangle$ obtained in Eq. (4) is used to calculate the probability of getting a coincidence count [31].

$$R_c \propto \int dt_1 \int dt_2 |\langle 0|E_2^{(+)}E_1^{(+)}|\psi\rangle|^2, \quad (5)$$

where the field at the detector D_1 can be written as

$$E_1^{(+)} = \int d\omega' e^{-[\omega'-\Omega_1]^2/\sigma_1^2} e^{-i\omega' t_1^o} a_o(\omega'), \quad (6)$$

where $t_1^o = t_1 - l_1^o/c$, l_1^o is the optical path length experienced by the o-polarized photon from the output face of the crystal to D_1 and $a_o(\omega')$ is the destruction operator of o-polarized photon of frequency ω'. Ω_1 is the central frequency and $\sigma_1^2 = 4\ln 2/[\sigma_1^{\mathrm{FWHM}}]^2$, where σ_1^{FWHM} is the FWHM bandwidth of the spectral filter inserted in front of the detector D_1. $E_2^{(+)}$ is defined similarly.

We now define the two-photon amplitude (or biphoton) as

$$A(t_+, t_-) = \langle 0|E_2^{(+)}E_1^{(+)}|\psi\rangle, \quad (7)$$

where $t_+ \equiv (t_1^o + t_2^e)/2$, and $t_- \equiv t_1^o - t_2^e$.

For generality, we have included the spectral filtering in Eq. (6). The effect of spectral filtering on the two-photon effective wave function in femtosecond-pulse-pumped type-II SPDC is studied theoretically and experimentally by Kim *et al* [32]. For the purpose of this paper, the bandwidths of the spectral filters σ_1 and σ_2 are now taken to be infinite. Let us also assume degenerate SPDC ($\Omega_1 = \Omega_2$).

Therefore the two-photon amplitude originated from each pump pulse has the form [23]

$$A(t_+, t_-) = e^{-i\Omega_p t_+}\int_{-\infty}^{\infty} d\nu_p \int_{-\infty}^{\infty} d\nu_- \int_0^L dz e^{-[\nu_p/\sigma_p]^2} \times e^{-i\{\nu_p D_+ + [\nu_-/2]D\}z} e^{-i\nu_p t_+} e^{-i[\nu_-/2]t_-},$$

$$\equiv e^{-i\Omega_p t_+}\Pi(t_+, t_-), \quad (8)$$

where $D_+ \equiv \frac{1}{2}\{1/u_o(\Omega_o) + 1/u_e(\Omega_e)\} - 1/u_p(\Omega_p)$, and $D \equiv 1/u_o(\Omega_o) - 1/u_e(\Omega_e)$. $u_o(\Omega_o)$ is the group velocity of a o-polarized photon of frequency Ω_o inside the BBO. Subscripts o, e, and p refer to o-polarized photon, e-polarized photon, and the pump, respectively. ν_p is the detuning from the pump central frequency Ω_p ($\nu_p = \omega_p - \Omega_p$). ν_o and ν_e are defined similarly and $\nu_- \equiv \nu_o - \nu_e$.

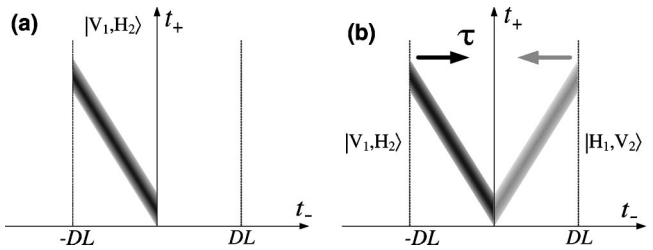

FIG. 2. (a) Biphoton wave function with femtosecond-pulse pump in the case of Fig. 1(a) is shown in density plot. It differs significantly from the case of cw pumped type-II SPDC. It starts at $-DL$ and ends at 0 due to the fact that a BBO is a negative uniaxial crystal so that the group velocity of the e polarization is greater than that of the o polarization. This figure shows how the two-photon amplitude $|V_1, H_2\rangle$ is distributed in time. (b) Two biphoton amplitudes ($|V_1, H_2\rangle$ and $|H_1, V_2\rangle$) are present in the case of the experimental setup shown in Fig. 1(b). When τ is increased, the two biphoton wave-functions move toward each other. If the pump is cw, the biphoton is essentially infinitely long in t_+ direction. If $\tau = DL/2$, in the case of cw-pumped type-II SPDC, the overlap is complete and 100% quantum interference can be observed. However, there is only limited amount of overlap due to the peculiar shape of the biphoton amplitudes in pulse-pumped type-II SPDC and this results in the reduction of the visibility of quantum interference. This is the inherent difference from cw pumped type-II SPDC.

The exact form of the $\Pi(t_+, t_-)$ function is given by

$$\Pi(t_+, t_-) = \begin{cases} g\, e^{-\sigma_p^2\{t_+ - [D_+/D]t_-\}^2/4} & \text{for } 0 < t_- < DL \\ 0 & \text{otherwise,} \end{cases}$$

where g is a constant. Note that, different from the cw case where Π is a function of t_- only [30], Π is now a function of both t_+ and t_-.

The shape of the $\Pi(t_+, t_-)$ function is shown in Fig. 2(a). It differs from the cw pumped type-II SPDC significantly. Similar to the cw case, the biphoton starts at $t_- = 0$ and ends at $|t_-| = DL$ [30], but unlike the cw case, there is a strong dependence on the t_+ direction. This is the reason why quantum interference visibility is reduced in femtosecond-pulse-pumped type-II SPDC.

To prepare a polarization entangled state using type-II collinear SPDC, one first has to replace the PBS in Fig. 1(a) with a nonpolarizing 50/50 beamsplitter (NPBS), see Fig. 1(b), so that there are two biphoton amplitudes to contribute to a coincidence count: (i) the signal is transmitted and the idler is reflected at the NPBS ($t-r$ or $|V_1, H_2\rangle$ amplitude), or (ii) the signal is reflected and the idler is transmitted at the NPBS ($r-t$ or $|H_1, V_2\rangle$ amplitude). Here we only considered the coincidence contributing amplitudes: amplitude postselection. When these two $t-r$ ($|V_1, H_2\rangle$) and $r-t$ ($|H_1, V_2\rangle$) amplitudes are made indistinguishable, a Bell state is prepared (modulo amplitude postselection) and it can be confirmed experimentally by observing 100% quantum interference [18]. To make the two amplitudes indistinguish-

able, the *e-o* delay τ should be correctly chosen. A typical method by which to find the correct *e-o* delay τ is to observe the interference dip (sometimes called the Hong-Ou-Mandel dip) when the *e-o* delay τ in Fig. 1(b) is varied. One then fixes τ where the complete destructive (when analyzers are set at $A_1=A_2=45°$) or constructive (when analyzers are set at $A_1=45°$ and $A_2=-45°$) interference occurs.

What happens in the experimental setup shown in Fig. 1(b) can be understood easily in the biphoton picture shown in Fig. 2(b). As discussed above, there are two biphoton amplitudes distributed in (t_+,t_-) space. The one on the left represents $|V_1,H_2\rangle$ and the one on the right represents $|H_1,V_2\rangle$. When the *e-o* delay $\tau=0$, there is no overlap, i.e, no quantum interference. As τ increases, the biphoton wave functions move toward each other by τ. In cw pumped type-II SPDC, when $\tau=DL/2$, the overlap between two amplitudes is complete since the biphoton amplitude is essentially independent of t_+, i.e., 100% quantum interference can be observed. On the other hand, in femtosecond-pulse-pumped type-II SPDC, as shown in Fig. 2(b), the amount of overlap is very small even at $\tau=DL/2$. Due to the tilted shape of the biphoton amplitude, there can never be 100% overlap between the two amplitudes and this results in the reduction of the visibility of quantum interference. It is important to note that, by introducing τ, we are shifting the biphoton amplitudes in the t_- direction only.

There are several ways to increase the overlap between the two biphoton amplitudes: (i) One can use a thin BBO crystal. In this case the relative area of overlap between the two biphoton amplitudes is increased (since $|DL|$ is decreased) by sacrificing the amount of photon flux. (ii) One can use very narrow-band spectral filters in front of the detectors. In this case, the biphoton amplitudes get broadened strongly in the t_- direction, which results in increased overlap between the two amplitudes [32]. (The effect of spectral filtering in t_+ direction is much smaller than that in t_- direction.) Again, the available photon flux is reduced.

Branning *et al.* recently introduced an interferometric technique to overcome this problem by placing a type-II BBO crystal in a Michelson interferometer [26]. Such a method can in principle give a 100% quantum interference. It, however, cannot be used to prepare a polarization Bell state since there are *four* biphoton amplitudes, rather than two, involved in the interfering process [27]. In addition, the first-order interference (observed in single counting rates) cannot be avoided in Branning *et al.*'s scheme [33]. Let us discuss this a little further. By placing a thick (5-mm) type-II BBO crystal into a Michelson interferometer, Branning *et al.* achieve a double-pass down-conversion scheme [34]. In this case, there are *four* biphoton amplitudes involved in the process: two from the first pass of the pump pulse and the other two from the second pass of the pump pulse since each pass of the pump pulse results in two biphoton amplitudes as shown in Fig. 2(b). Then the nonzero contribution of the biphoton amplitudes in Branning *et al.*'s scheme can be depicted as in Fig. 3. T_p is the delay introduced between the first pass and the second pass of the pump pulse, i.e., the delay between the two biphoton amplitudes from the first

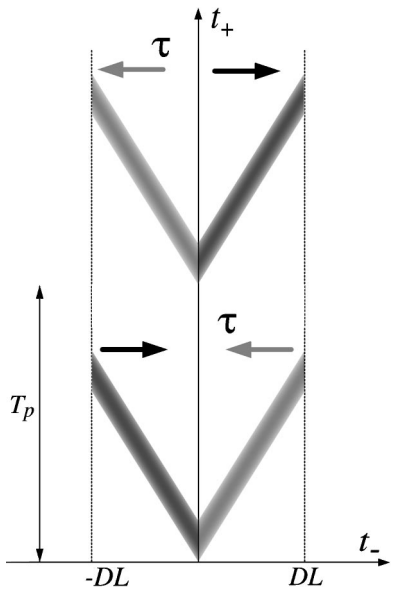

FIG. 3. Biphoton amplitudes for Branning *et al.*'s scheme. Four amplitudes are involved in the quantum interference, two from the first pass of the pump pulse (upper diagram) and two from the second pass of the pump pulse (lower diagram). The delay between the amplitudes from the first pass and the second pass is T_p. τ is the same *e-o* delay shown in Fig. 1(b). The direction of arrows represent how the relevant amplitudes moves in the t_- direction when τ is increased.

pass of the pump pulse and the two biphoton amplitudes from the second pass of the pump pulse. This delay T_p is only introduced in the t_+ direction [35,36]. The *e-o* delay τ is introduced in the t_- direction by introducing a stack of quartz plates as before, see Figs. 1(b) and 2(b). When $\tau=0$ and $T_p=0$, 100% quantum interference should be observed if polarization information is erased by setting both analyzers at 45°. However, Bell states of the type shown in Eq. (1) have not been prepared in this method.

Let us now consider the experimental setup shown in Fig. 4 [37]. A type-II BBO crystal is placed in each arm of the Mach-Zehnder interferometer (MZI). The pump pulse is polarized at 45° by using a $\lambda/2$ plate. PBS is the polarizing beamsplitter. The optic axis of the first BBO is oriented vertically ($\updownarrow$) and the other horizontally ($\odot$). The pump pulse is blocked by the mirrors M_3 and M_4. There are only two biphoton amplitudes in this process, one from each crystal, due to the fact that a polarizing beamsplitter is used to split the signal and the idler of the entangled photon pairs. Therefore, the quantum state, when the MZI is properly aligned, can be written as

$$|\psi\rangle=|H_1,V_2\rangle+e^{i\varphi}|V_1,H_2\rangle, \tag{9}$$

where H and V represent horizontal and vertical polarization respectively. Therefore, by varying the relative phase delay φ, one can prepare the Bell states $|\Psi^{\pm}\rangle$. The other two Bell states $|\Phi^{\pm}\rangle$ can be easily achieved by inserting a $\lambda/2$ plate in one output port of the MZI. Note that $\varphi=\Omega_p T_p$, where T_p is the time delay between the two amplitudes in Eq. (9), so that by varying T_p, modulation in the coincidence counting rate

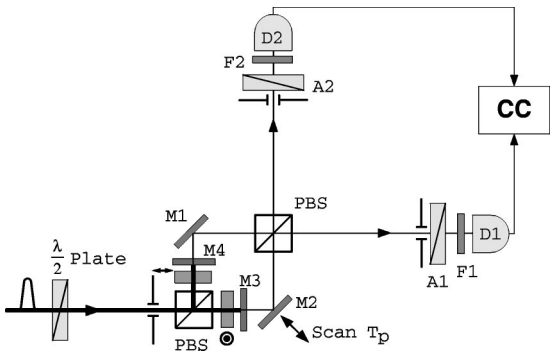

FIG. 4. Bell-state preparation scheme using two type-II BBO in a Mach-Zehnder interferometer. T_p is the delay between the biphoton amplitudes from two different crystals. The relative phase is between the two amplitudes delay, $\varphi=\Omega_p T_p$. Note that the optic axes of the BBO crystals are oriented orthogonally, one vertically ($\updownarrow$) and the other horizontally ($\odot$). See text for detail.

is observed at the pump central frequency. Therefore, in this scheme, a true Bell state can be prepared without any post-selection methods. As we shall show later in this section, the thickness of the nonlinear crystals and the spectral filtering of the entangled photon flux do not affect the visibility in principle, even with a femtosecond-pulse pump.

In this configuration, *e*-polarized photons are always detected by D_2 and *o*-polarized photons are always detected by D_1. This is of great importance when the femtosecond laser is used as a pump. The biphoton amplitude for each coincidence detection event is shown in Fig. 5. Note that only two biphoton amplitudes are involved in the quantum interference. If the MZI is balanced, 100% quantum interference can be observed. This scheme provides a good method of preparing Bell states. If a cw pump is used instead [38], it is not absolutely necessary to have the optic axes of the crystals

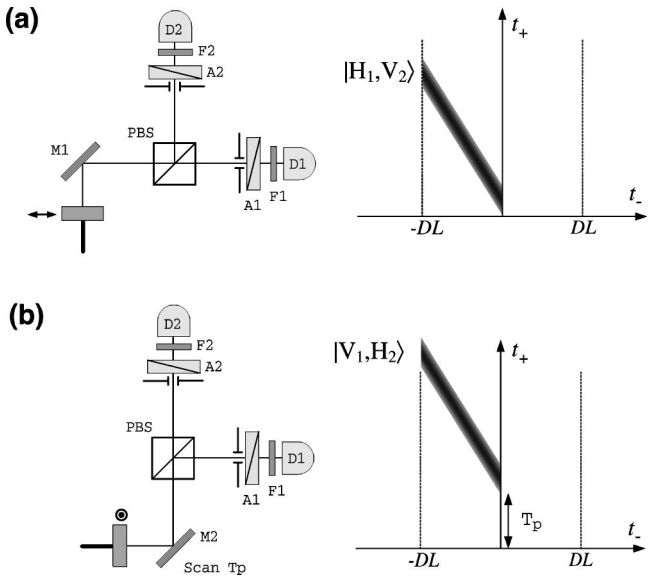

FIG. 5. This figure illustrates the two interfering biphoton amplitudes in the experimental setup shown in Fig. 4. T_p is the time delay between the two biphoton amplitudes. If the MZI is balanced, i.e., $T_p=0$, complete overlap can be achieved.

orthogonally oriented. Suppose that the optic axis of the crystal in Fig. 5(b) is now oriented vertically ($\updownarrow$), then the corresponding biphoton amplitude will appear flipped about $t_-=0$, thus appearing from 0 to DL. Clearly, there cannot be any overlap between two amplitudes even with the balanced MZI ($T_p=0$), just as the case considered in Figs. 1(b) and 2(b). However, in the cw pump case, the biphoton amplitudes are independent of t_+. Therefore, by making appropriate compensation in the t_- direction, the two amplitudes can be overlapped, i.e., by setting the *e-o* delay $\tau=DL/2$. Note that if the coherence length of the cw pump laser is not long enough, then perfect overlap cannot be obtained for the same reason as in the femtosecond-pulse-pumped case.

So far, we have pictorially shown that a true Bell state can be obtained in femtosecond-pulse-pumped type-II SPDC by using an interferometric technique. The picture we have presented is based on the biphoton amplitude calculated earlier in this section. The space-time and polarization interference effects are calculated as follows. We use the right-hand coordinate system assuming the direction of propagation as the *z* axis. Then the sum of biphoton amplitudes in the experimental scheme, Fig. 4, is,

$$\begin{aligned}\mathcal{A}(t_+,T_p,t_-)&=(\hat{e}_1\cdot\hat{e}_H)(\hat{e}_2\cdot\hat{e}_V)e^{-i\Omega_p t_+}\Pi(t_+,t_-)\\&\quad+(\hat{e}_1\cdot\hat{e}_V)(\hat{e}_2\cdot\hat{e}_H)\\&\quad\times e^{-i\Omega_p(t_++T_p)}\Pi(t_++T_p,t_-),\end{aligned}\tag{10}$$

where $\hat{e}$ represents the unit vector in a certain direction, for example, $\hat{e}_1$ represents the direction of the analyzer A_1. The coincidence counting rate is then calculated as

$$\begin{aligned}R_c&=\int dt_+dt_-|\mathcal{A}(t_+,T_p,t_-)|^2\\&=\int dt_+dt_-|\sin\theta_1\cos\theta_2\Pi(t_+,t_-)\\&\quad+\cos\theta_1\sin\theta_2 e^{-i\Omega_p T_p}\Pi(t_++T_p,t_-)|^2\\&\propto\sin^2\theta_1\cos^2\theta_2+\cos^2\theta_1\sin^2\theta_2\\&\quad+2V(T_p)\cos(\Omega_p T_p)\sin\theta_1\cos\theta_2\cos\theta_1\sin\theta_2,\end{aligned}\tag{11}$$

where

$$V(T_p)\equiv\frac{\int dt_+dt_-\Pi(t_+,t_-)\Pi(t_++T_p,t_-)}{\int dt_+dt_-\Pi^2(t_+,t_-)}=e^{-[\sigma_p T_p]^2/8}.\tag{12}$$

Therefore, the space-time interference at $\theta_1=\theta_2=45°$ will show

$$R_c = 1 + V(T_p)\cos(\Omega_p T_p), \tag{13}$$

and the polarization interference will show

$$R_c = \sin^2(\theta_1 + \theta_2) \quad \text{for} \quad \Omega_p T_p = 0. \tag{14}$$

It is important to note that the envelope of the space-time interference, when no spectral filters are used, $V(T_p)$ function, is exactly equal to that of the self-convolution of the pump pulse. No crystal parameters affect the envelope of the space-time interference pattern. As we shall show in Sec. IV, this is a special feature of type-II SPDC. If any spectral filtering is used, naturally, the envelope will be broadened.

III. BELL-STATE PREPARATION USING TYPE-II SPDC: EXPERIMENT

As mentioned before, the goal of this section is to experimentally demonstrate that high-visibility quantum interference, which can be used to prepare a two-photon polarization Bell state, can be observed in the experimental scheme shown in Fig. 4 and the envelope of these interference fringes is exactly the same as the pump pulse envelope.

Let us first discuss the experimental setup, see Fig. 4. As briefly discussed in Sec. II, a type-II BBO crystal is placed in each arm of the MZI and the optic axes of the crystals are oriented orthogonally, one vertically ($\updownarrow$) and the other horizontally ($\odot$). The thickness of the crystals is 3.4 mm each. The crystals are pumped by frequency-doubled (by using a 700-μm type-I BBO) radiation of a Ti:Sa laser oscillating at 90 MHz. The pump has the central wavelength of 400 nm. The average power of the laser beam in each arm of the MZI is approximately 10 mW. The residual pump-laser beam is blocked by two mirrors M_3 and M_4 and the relative phase $\varphi = \Omega_p T_p$ between the two amplitudes can be varied by adjusting one of the mirrors M_2. Collinear degenerate down conversion is selected by a set of pinholes.

We first measure the envelope of the pump pulse itself by blocking the SPDC photons while detecting a small fraction of the pump light that passed through the mirrors M_3 and M_4. This is done by simply using another set of interference filters that transmit 400 nm radiation. Figure 6 shows the measured envelope of the pump pulse interference patters. The measured FWHM is 170 fs and this will be compared with the envelope of the two-photon quantum interference patterns.

The space-time quantum interference is observed at $\theta_1 = \theta_2 = 45°$ by varying T_p. Two sets of experimental data are collected by using two different sets of interference filters, FWHM bandwidths of 10 nm and 40 nm with 800-nm central wavelength, to demonstrate the effect of spectral filtering on the biphoton wave-function. A 3-nsec coincidence window is used and single counting rates of the detectors are recorded as well.

Figure 7 shows the data for these two measurements. In Fig. 7(a), the FWHM of the interference envelope is 310 fs. This shows that 10-nm filter has some effect on the shape of the biphoton wave function. This is not so surprising since the FWHM bandwidth of the SPDC spectrum for 3.4-mm

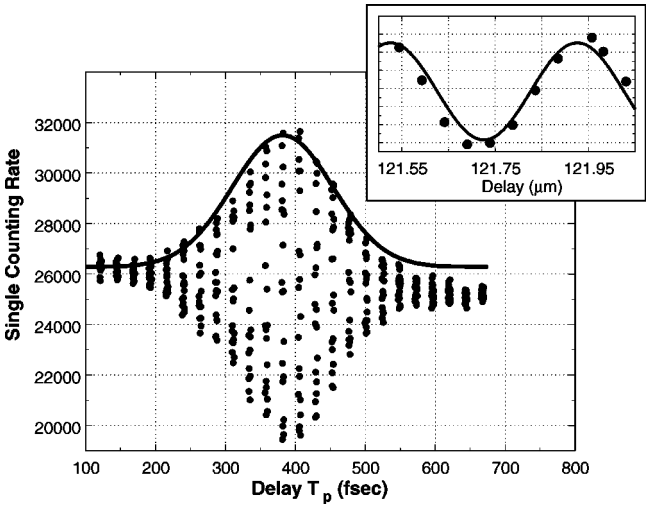

FIG. 6. Observed pump pulse interference by blocking the SPDC photons. The solid line is a Gaussian fit to the envelope. The FWHM of the pump pulse envelope measured from the Gaussian fit is 170 fs. Each column of data represents the modulation of about one wavelength and the modulation period is 400 nm as shown in the inset. The inset has the same vertical scale as the main figure and the delay is displayed in μm (rather than in fs) to clearly show the modulation period. The inset shows the detailed modulation around $T_p \approx$ 406 fs.

BBO is 3 nm. However, when 40-nm filters are used, see Fig. 7(b), the FWHM of the envelope (170 fs) is equal to the FWHM of the pump pulse interference patterns, see Fig. 6. The effects of the spectral filters are not present and Eq. (13) is confirmed experimentally. The average visibility is 76%, which is higher than in any femtosecond-pulse-pumped type-II SPDC experiments with a thick crystal and no spectral filters. No interference is observed in the single detector counting rates.

The visibility loss is mostly due to the imperfect alignment of the system. Due to the anisotropy of the BBO crystal, the *e* ray walks off from the beam path of the *o* ray. Although both *e* rays from the two different crystals are collected at the same detector, the walk off is in different directions: one walks off horizontally, the other walks off vertically. When thick crystals are used, 3.4 mm in our case, such an effect is not negligible [39]. Since we are not interested in making any filtering, spectral or spatial, spatial filtering using a single mode fiber is not desirable. Instead of using spatial filtering, such a walk off can be removed in another way: the two crystals are oriented in the same direction and then insert a $\lambda/2$ plate after one of the crystals [38].

The interferometry using the MZI, however, has one disadvantage, keeping the phase coherence between the two arms of the interferometer over a long time can be difficult. Although we have shown here that the visibility can be improved and in principle reach 100%, if the phase coherence is not kept for a long time, such a method is not useful as a source of Bell states for other experiments. We now turn our attention to type-I SPDC and investigate whether it offers a good solution to this problem. As we shall show, type-I

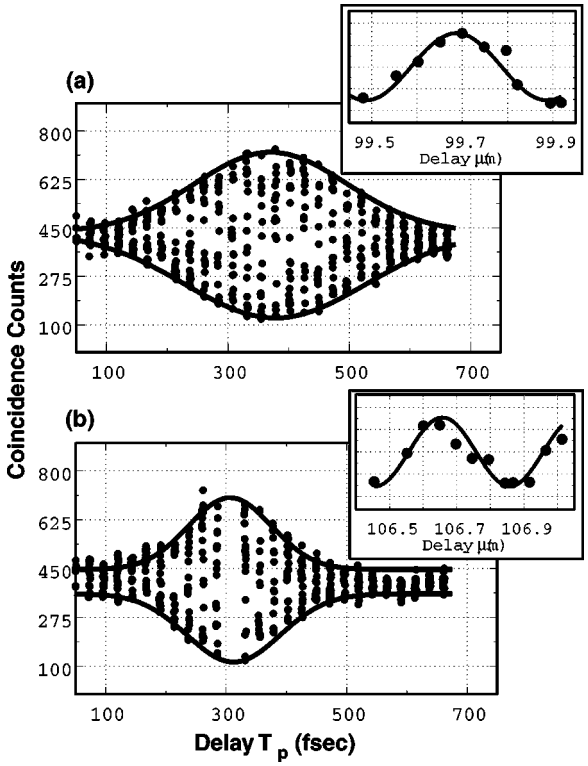

FIG. 7. Quantum interference observed with the experimental setup shown in Fig. 4. (a) 10-nm filters are used. Accumulation time is 60 s. The measured width of the envelope is approximately 310 fs. The visibility is $\approx$ 75%. (b) 40 nm filters are used. Accumulation time is 80 s. The measured FWHM of the envelope is $\approx$170 fs, which is equal to the FWHM envelope of the pump pulse itself. The visibility is $\approx$ 76%. Each column of data represent the modulation of about one wavelength with a modulation period of 400 nm as predicted in Eq. (13). The insets have the same vertical scales as the main figures and they show the detailed modulations around (a) $T_p \approx 332$ fs and (b) $T_p \approx 356$ fs.

SPDC offers a better way of preparing Bell states in femtosecond-pulse-pumped SPDC.

IV. BELL-STATE PREPARATION USING TYPE-I SPDC: THEORY

In this section, we discuss how one can prepare a polarization Bell state in an interferometric way using *degenerate* type-I SPDC pumped by a femtosecond-pulse pump.

In general, the difference between type-II SPDC and type-I SPDC stems from calculating the phase mismatch term Δ in Eq. (4). In type-II SPDC, due to the fact that the signal and the idler photons have orthogonal polarization, only the first-order Taylor expansion of Δ is necessary, even in degenerate case. In degenerate type-I SPDC, however, one has to go to the second-order expansion since the first-order terms cancel if the frequencies are degenerate. Therefore, nondegenerate type-I SPDC formalism is basically the same as that of degenerate type-II SPDC and we will not discuss it here again. On the other hand, as we shall show, degenerate

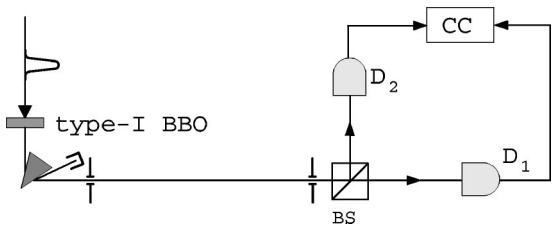

FIG. 8. Most simple two-photon correlation experiment using type-I SPDC. See text for detail.

type-I SPDC differs quite a lot from type-II SPDC or nondegenerate type-I SPDC.

Let us first consider the experimental situation shown in Fig. 8. Type-I SPDC occurs in the crystal and the photon pairs are detected by two detectors D_1 and D_2. The state of type-I SPDC is the same as Eq. (4) except that both photons are now *o* polarized. For type-I degenerate SPDC, the phase mismatch term Δ becomes

$$\Delta = -\left(\nu_p D_+ + \frac{1}{4}\nu_-^2 D'' \right), \tag{15}$$

where $\nu_- = \nu_i - \nu_s$ and subscripts *p*, *i*, and *s* refer to the pump, idler, and the signal, respectively. $D_+ = 1/u_o(\Omega_p/2) - 1/u_p(\Omega_p)$ where u_o (u_p) are the group velocities of the *o*-polarized photon (the pump photon) inside the crystal and $D'' = d^2K_o/d\Omega^2|_{\Omega=\Omega_p/2}$, where the wave vector $K_o = \Omega n_o(\Omega)/c$. $n_o(\Omega)$ is the index of refraction of the crystal for a given frequency Ω. Note that D_+ is defined differently from the type-II SPDC case.

Therefore, the biphoton amplitude $A(t_+,t_-)$ for type-I SPDC now becomes [23]

$$\begin{aligned} A(t_+,t_-) &= e^{-i\Omega_p t_+}\int_{-\infty}^{\infty} d\nu_p \int_{-\infty}^{\infty} d\nu_- \int_0^L dz e^{-[\nu_p/\sigma_p]^2} \\ &\quad \times e^{-i[\nu_p D_+ + \nu_-^2 D''/4]z} e^{-i\nu_p t_+} e^{-i[\nu_-/2]t_-}, \\ &\equiv e^{-i\Omega_p t_+}\Pi(t_+,t_-), \end{aligned} \tag{16}$$

where

$$\Pi(t_+,t_-) = \int_0^L dz \frac{1}{\sqrt{z}} e^{-\sigma_p^2[t_+ + D_+ z]^2/4} e^{it_-^2/[4D''z]}. \tag{17}$$

Unlike the pulse pumped type-II SPDC, the $\Pi(t_+,t_-)$ function is symmetric in t_-. To simplify the calculation, no spectral filters are assumed.

Having calculated the effective biphoton wave function of type-I SPDC, let us now consider the experimental scheme shown in Fig. 9 and calculate the coincidence counting rate in detail. Two interfering amplitudes are created from the two crystals similar to Fig. 5 except that the biphoton ampli-

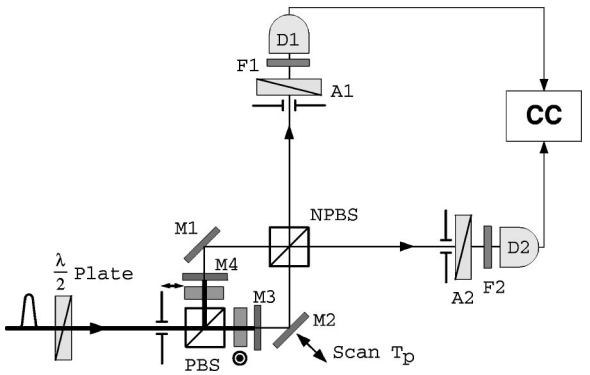

FIG. 9. Experimental scheme for two type-I crystals. Now, a type-I BBO crystal is placed in each arm of the MZI and the optic axes are orthogonally oriented. The output beamsplitter (NPBS) of the MZI is now 50/50 nonpolarizing beamsplitter.

tudes now look different in type-I SPDC. In the single-mode approximation, the quantum state prepared in the experimental setup of Fig. 9 is given by

$$|\psi\rangle = |V_1, V_2\rangle + e^{i\varphi}|H_1, H_2\rangle, \tag{18}$$

where φ is the relative phase between two amplitudes. If the phase φ is correctly chosen, the Bell states $|\Phi^{\pm}\rangle$ can be prepared. (Note also that by inserting a $\lambda/2$ plate in one output port of the NPBS, the other two Bell states $|\Psi^{\pm}\rangle$ can also be prepared.) As we shall show below, there is no need for any spectral postselection in this case, however, amplitude postselection is assumed because there are possibilities that the signal and the idler exit at the same output port of the beamsplitter. This event, however, is not detected since we only consider the coincidence contributing events. Such amplitude postselection is not desirable in principle. Luckily, there is a way to get around this problem, which we shall briefly discuss in Sec. V.

Let us now calculate the coincidence counting rates for the experimental setup shown in Fig. 9 using the biphoton amplitude calculated in Eq. (16). By using the right-hand coordinate system as in the type-II SPDC case, the coincidence counting rate is given by

$$\begin{aligned} R_c \propto & \int dt_+ dt_- |-\sin\theta_1 \sin\theta_2 \Pi(t_+, t_-) + \cos\theta_1 \cos\theta_2 \\ & \times e^{-i\Omega_p T_p} \Pi(t_+ + T_p, t_-)|^2 \\ = & \sin^2\theta_1 \sin^2\theta_2 + \cos^2\theta_1 \cos^2\theta_2 \\ & - 2G(T_p)\cos(\Omega_p T_p)\sin\theta_1 \sin\theta_2 \cos\theta_1 \cos\theta_2, \end{aligned} \tag{19}$$

where $G(t) = g(t)/g(0)$ with

$$g(t) = \int dt_+ dt_- \Pi(t_+, t_-)\Pi^*(t_+ + t, t_-).$$

The $G(t)$ function gives the envelope of the quantum interference pattern as a function of t.

Therefore, the space-time interference at $\theta_1 = \theta_2 = 45°$ will show

$$R_c = 1 - G(T_p)\cos(\Omega_p T_p), \tag{20}$$

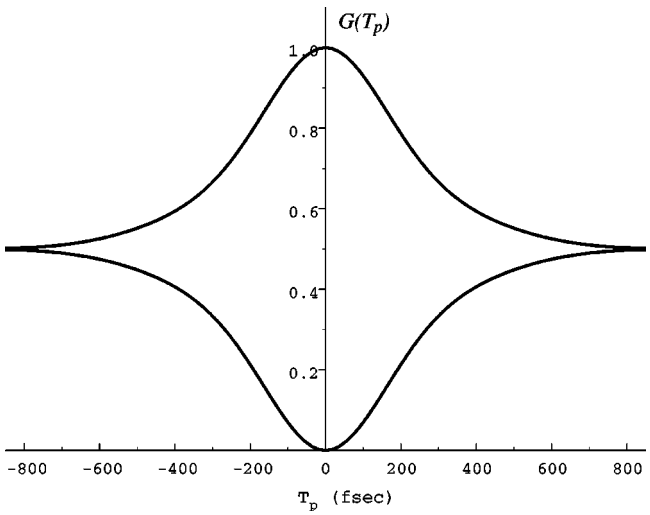

FIG. 10. Calculated envelope of the interference pattern $G(T_p)$ from Eq. (22) for the experimental parameters in our experiment. Note that there are long tails of the interference envelope.

and the polarization interference will show

$$R_c = \cos^2(\theta_1 + \theta_2) \quad \text{for} \quad \Omega_p T_p = 0. \tag{21}$$

The envelope function of type-I SPDC, $G(T_p)$, differs a lot from that of the type-II SPDC, $V(T_p)$. $g(T_p)$ is calculated to be

$$\begin{aligned} g(T_p) = & \int_{-\infty}^{\infty} dt_+ \int_{-\infty}^{\infty} dt_- \Pi(t_+, t_-)\Pi^*(t_+ + T_p, t_-) \\ = & \int_0^1 du_1 \int_0^1 du_2 \int_{-\infty}^{\infty} dt_+ \int_{-\infty}^{\infty} dt_- \\ & \times e^{-\sigma_p^2 [t_+ + D_+ L u_1^2]^2/4} e^{i t_-^2/[4D'' L u_1^2]} \\ & \times e^{-\sigma_p^2 [t_+ + T_p + D_+ L u_2^2]^2/4} e^{-i t_-^2/[4D'' L u_2^2]} \\ = & C \int_0^1 du_1 \int_0^1 du_2 \frac{u_1 u_2}{\sqrt{|u_1^2 - u_2^2|}} e^{-\sigma_p^2 \{D_+ L [u_1^2 - u_2^2] - T_p\}^2/8}, \end{aligned} \tag{22}$$

where C is a constant and the change of variable, $z_i = u_i^2 L$ $(i = 1,2)$, has been made.

It is interesting to find that the envelope function $G(T_p)$ *does not* explicitly contain the second-order expansion of the phase mismatch term D'' at all. This result is quite surprising since the presence of D'' is the principal difference between type-II SPDC and the degenerate type-I SPDC. (This is due to the fact that $D = 0$ for degenerate type-I SPDC.) Note also that the envelope of the space-time interference is not simply that of the convolution of the pump pulse as in type-II SPDC shown in Eq. (13); it is a complicated function of $D_+ L$ and σ_p. Figure 10 shows $G(T_p)$ when realistic experimental parameters are substituted in Eq. (22).

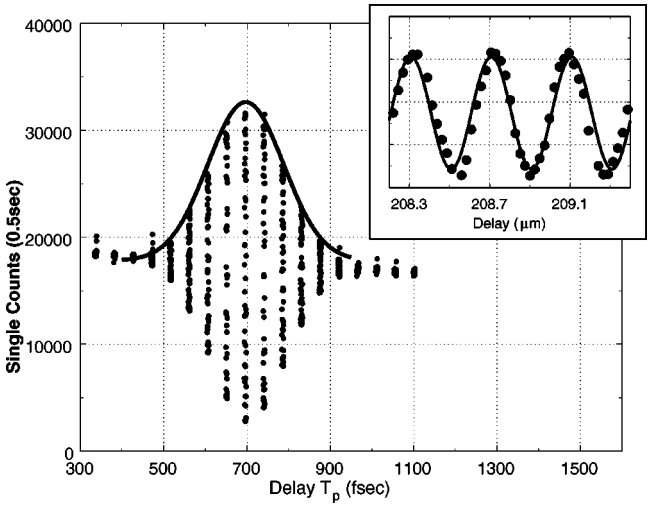

FIG. 11. Pump pulse interference. The measured FWHM envelope is approximately 200 fs. Solid line is the Gaussian fit to the envelope. Each column of data represents the modulation of several wavelengths with modulation period of 400 nm as shown in the inset. The inset has the same vertical scale as the main figure and it shows the detailed modulation around $T_p \approx 696$ fs.

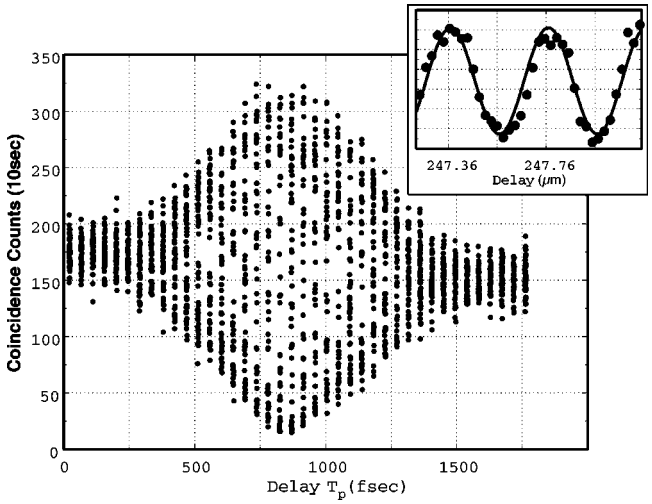

FIG. 12. Space-time interference observed in coincidence between the two detectors D_1 and D_2 for the analyzer setting $\theta_1 = \theta_2 = 45°$. 10-nm filters are used for this measurement. Note that the FWHM is much bigger than the pump pulse interference shown in Fig. 11. 400-nm modulation is observed as predicted in Eq. (20). The inset has the same vertical scale as the main figure and it shows the detailed modulation around $T_p \approx 826$ fs.

V. ''BELL-STATE PREPARATION USING TYPE-I SPDC EXPERIMENT''

In the experiment, we use two pieces of type-I BBO crystal cut for collinear degenerate SPDC. The thickness of the crystals is 3.4 mm each. The pump pulse central wavelength is 400 nm and the average power of the pump beam in each arm of the MZI is approximately 10 mW as in the type-II experiment. The repetition rate of the pump pulse is approximately 82 MHz.

We first measured the pump pulse envelope. The BBO crystals are not removed from the MZI for the pump pulse envelope measurement. This data is shown in Fig. 11. Gaussian fitting of the data gives the FWHM equal to 200 fs. This is to be compared with the envelope of the quantum interference pattern measured in coincidence counting rate between the two detectors D_1 and D_2.

To observe the quantum interference, we first block all the residual pump radiation using additional absorption filters. Analyzer angles are set at $\theta_1 = \theta_2 = 45°$. The interference filters used in this measurement have 10 nm bandwidth. As expected, high-visibility quantum interference is observed, see Fig. 12. The FWHM of the interference envelope is much bigger than that of the pump pulse itself, see Fig. 11. Unfortunately, due to rather large fluctuations in the data, long tails of the interference envelope predicted by Eq. (22), see Fig. 10, are washed out.

With 40-nm filters, the shape of the envelope remained almost the same, while the width of the envelope and the visibility is slightly reduced. The reduction of the visibility with 40-nm filters is mainly due to the difficulty in aligning both crystals with broadband filters.

There are two problems with this method: (i) amplitude postselection is assumed, and (ii) the MZI cannot be made very stable for a long term. In a recently published paper [40], the second problem was solved by using the ''collinear interferometer'' method in which two type-I crystals are placed collinearly with the optic axes orthogonally oriented. The first problem, amplitude postselection, was also removed by employing *nondegenerate* type-I SPDC in the collinear scheme [41]. Also with collinear method, aligning the crystals is much easier and the visibility as high as 92% was easily obtained with 40-nm filters [40]. Although the collinear method and the MZI method look different, the theoretical description we have presented in the previous sections applies with no modifications. The theory described in Sec. IV explains all the experimental results of Ref. [40] in detail and the experimental results shown in Ref. [41] can be explained by using the theory described in Sec. II by exchanging the polarization label with the frequency label.

VI. CONCLUSION

We have shown that high-visibility quantum interference can be observed without using narrow-band filters for both type-II and type-I SPDC pumped by femtosecond laser pulses. In these methods, a Mach-Zehnder interferometer is used to coherently add two biphoton amplitudes from two different nonlinear crystals pumped by coherent laser pulses. Using this method, maximally entangled two-photon polarization states, or Bell states, can be successfully prepared.

It is important to note that biphoton or two-photon amplitudes generated from coherent pump laser *remain coherent* even though they may originate from different spatial [35] or temporal [32,36,42] domains. As long as the distinguishing information present in the interfering amplitudes are erased, high-visibility quantum interference should be observed.

There is, however, one problem with the method using a Mach-Zehnder interferometer: keeping the phase coherence

is difficult. This is a rather serious problem especially when one is interested in using such a method to prepare a Bell state and use it as a source. The collinear two-photon interferometer solves this problem. In this method, two type-I crystals are placed collinearly in the pump beam path [40,41]. Although different geometry is used, the theory presented in Secs. II and IV applies equally for both the Mach-Zehnder interferometer and the collinear case.

For the two-crystal scheme using pulse pumped type-II SPDC, the envelope of the space-time interference pattern is determined only by the bandwidth of the pump pulse σ_p, as shown in Secs. II and III. Crystal parameters do not affect the envelope of the interference pattern at all. On the other hand, for the two-crystal scheme using pulse pumped type-I SPDC, the envelope of the interference pattern strongly depends on the crystal parameters, especially on $D_+ = 1/u_o(\Omega_p/2) - 1/u_p(\Omega_p)$ and the crystal thickness L as well as the pump bandwidth σ_p, as shown in Secs. IV and V. It is also interesting to note that the envelope of the interference pattern does not have explicit dependence on D''.

It is important to note the following. To observe the space-time interference, one can introduce the delay in two ways: (i) in t_- or (ii) in t_+. In the single-crystal SPDC scheme, quantum interference is observed by introducing the delay τ in t_-. But in the two-crystal SPDC scheme, one can introduce either in t_- or in t_+. In this paper, we have demonstrated high-visibility quantum interference in femtosecond-pulse-pumped SPDC by introducing a delay T_p in t_+.

In conclusion, we have demonstrated Bell-state preparation schemes using femtosecond pulse-pumped SPDC. In type-II SPDC, the envelope of the interference pattern is exactly equal to the envelope of the pump pulse convolution. On the other hand, the envelope of interference pattern from type-I SPDC is much broader than that of the pump interference. This may be useful if one needs to use femtosecond-pulse-pumped SPDC, yet requires that two-photon amplitudes are distributed in time more than the pump pulse itself. Type-I SPDC has an advantage over type-II SPDC; two crystals can be easily used collinearly. As demonstrated in Refs. [40,41], such a method will serve as a good source of entangled photon pairs for experiments, which require accurate timing to overlap biphotons from different domains.

ACKNOWLEDGMENTS

We would like to thank V. Berardi and L.-A. Wu for their help during the last part of the experiment. This research was supported, in part, by the Office of Naval Research, ARDA and the National Security Agency.

[1] E. Schrödinger, Naturwissenschaften **23**, 807 (1935); **23**, 823 (1935); **23**, 844 (1935); the English translation appears in *Quantum Theory and Measurement*, edited by J.A. Wheeler and W.H. Zurek (Princeton University, New York, 1983).

[2] A. Einstein, B. Podolsky, and N. Rosen, Phys. Rev. **47**, 777 (1935).

[3] D. Bohm, *Quantum Theory* (Prentice-Hall Inc., New York, 1951).

[4] J.S. Bell, *Speakable and Unspeakable in Quantum Mechanics* (Cambridge University, New York, 1987).

[5] S.J. Freedman and J.F. Clauser, Phys. Rev. Lett. **28**, 938 (1972); J.F. Clauser and A. Shimony, Rep. Prog. Phys. **41**, 1881 (1978).

[6] A. Aspect, P. Grangier, and G. Roger, Phys. Rev. Lett. **47**, 460 (1981); A. Aspect, J. Dalibard, and G. Roger, *ibid.* **49**, 1804 (1982); A. Aspect, P. Grangier, and G. Roger, *ibid.* **49**, 91 (1982).

[7] C.O. Alley and Y.H. Shih, in *Proceedings of the 2nd International Symposium on Foundations of Quantum Mechanics*, edited by M. Namiki (Physical Society of Japan, Tokyo, 1986); Y.H. Shih and C.O. Alley, Phys. Rev. Lett. **61**, 2921 (1988).

[8] J.G. Rarity and P.R. Tapster, Phys. Rev. Lett. **64**, 2495 (1990); G. Weihs, T. Jennewein, C. Simon, H. Weinfurter, and A. Zeilinger, *ibid.* **81**, 5039 (1998).

[9] T. Jennewein, C. Simon, G. Weihs, H. Weinfurter, and A. Zeilinger, Phys. Rev. Lett. **84**, 4729 (2000); D.S. Naik, C.G. Peterson, A.G. White, A.J. Berglund, and P.G. Kwiat, *ibid.* **84**, 4733 (2000); W. Tittel, J. Brendel, H. Zbinden, and N. Gisin, *ibid.* **84**, 4737 (2000).

[10] C.H. Bennett, G. Brassard, C. Crépeau, R. Jozsa, A. Peres, and W.K. Wootters, Phys. Rev. Lett. **70**, 1895 (1993); D. Bouwmeester, J.-W. Pan, M. Eibl, H. Weinfurter, and A. Zeilinger, Nature (London) **390**, 575 (1997); D. Boschi, S. Branca, F. De Martini, L. Hardy, and S. Popescu, Phys. Rev. Lett. **80**, 1121 (1998); A. Furusawa, J.L. Sørensen, S.L. Braunstein, C.A. Fuchs, H.J. Kimble, and E.S. Polzik, Science **282**, 706 (1998); Y.-H. Kim, S.P. Kulik, and Y.H. Shih, Phys. Rev. Lett. **86**, 1370 (2001).

[11] D.N. Klyshko, *Photons and Nonlinear Optics* (Gordon and Breach, New York, 1988).

[12] D.N. Klyshko, Pis'ma Zh. Eksp. Teor. Fiz. **6**, 490 (1967) [JETP Lett. **6**, 23 (1967)].

[13] Ya.B. Zel'dovich and D.N. Klyshko, Pis'ma Zh. Éksp. Teor. Fiz. **9**, 69 (1969) [JETP Lett. **9**, 40 (1969)].

[14] D.C. Burnham and D.L. Weinberg, Phys. Rev. Lett. **25**, 84 (1970).

[15] D.N. Klyshko, Kvant. Elektron. (Moscow) **4**, 1056 (1977) (1977) [Sov. J. Quantum Electron. **7**, 591 (1977)]; M.F. Vlasenko, G.Kh. Kitaeva, and A.N. Penin, *ibid.* **7**, 441 (1980) [*ibid.* **10**, 252 (1980)].

[16] D.N. Klyshko, Kvant. Electron. (Moscow) **7**, 1932 (1980) [Sov. J. Quantum Electron. **10**, 1112 (1980)]; A.A. Malygin, A.N. Penin, and A.V. Sergienko, Pis'ma Zh. Éksp. Teor. Fiz. **33**, 493 (1981) [JETP Lett. **33**, 477 (1981)]; J.G. Rarity, K.D. Ridley, and P.R. Tapster, Appl. Opt. **26**, 4616 (1987).

[17] C.K. Hong, Z.Y. Ou, and L. Mandel, Phys. Rev. Lett. **59**, 2044 (1987).

[18] Y.H. Shih and A.V. Sergienko, Phys. Lett. A **186**, 29 (1994); **191**, 201 (1994).

[19] L. De Caro and A. Garuccio, Phys. Rev. A **50**, R2803 (1994).

[20] P.G. Kwiat, K. Mattle, H. Weinfurter, A. Zeilinger, A.V. Sergienko, and Y.H. Shih, Phys. Rev. Lett. **75**, 4337 (1995).
[21] P.G. Kwiat, E. Waks, A.G. White, I. Appelbaum, and P.H. Eberhard, Phys. Rev. A **60**, R773 (1999).
[22] A.V. Burlakov, M.V. Chekhova, O.A. Karabutova, D.N. Klyshko, and S.P. Kulik, Phys. Rev. A **60**, R4209 (1999); A.V. Burlakov and D.N. Klyshko, Pis'ma. Zh. Éksp. Teor. Fiz. **69**, 795 (1999) [JETP Lett. **69**, 839 (1999)].
[23] T.E. Keller and M.H. Rubin, Phys. Rev. A **56**, 1534 (1997).
[24] A.V. Sergienko, M. Atatüre, Z. Walton, G. Jaeger, B.E.A. Saleh, and M.C. Teich, Phys. Rev. A **60**, R2622 (1999).
[25] W.P. Grice and I.A. Walmsley, Phys. Rev. A **56**, 1627 (1997); G. Di Giuseppe, L. Haiberger, F. De Martini, and A.V. Sergienko, *ibid.* **56**, R21 (1997); W.P. Grice, R. Erdmann, I.A. Walmsley, and D. Branning, *ibid.* **57**, R2289 (1998).
[26] D. Branning, W.P. Grice, R. Erdmann, and I.A. Walmsley, Phys. Rev. Lett. **83**, 955 (1999); Phys. Rev. A **62**, 013814 (2000).
[27] It should be noted that Branning *et al.* do not claim Bell-state preparation in Ref. [26]. In this paper, we simply point out that the experimental scheme demonstrated in Ref. [26] cannot be used to prepare a Bell state, which is of interest to us.
[28] M. Atatüre, A.V. Sergienko, B.E.A. Saleh, and M.C. Teich, Phys. Rev. Lett. **84**, 618 (2000).
[29] Y.-H. Kim, S.P. Kulik, M.H. Rubin, and Y.H. Shih, Phys. Rev. Lett. (to be published).
[30] M.H. Rubin, D.N. Klyshko, Y.H. Shih, and A.V. Sergienko, Phys. Rev. A **50**, 5122 (1994).
[31] R.J. Glauber, Phys. Rev. **130**, 2529 (1963).
[32] Y.-H. Kim, V. Berardi, M.V. Chekhova, A. Garuccio, and Y.H. Shih, Phys. Rev. A **62**, 043820 (2000).
[33] The presence of the first-order interference in Branning *et al.*'s scheme is not surprising. Similar effects are already observed by many authors, see Refs. [32,35,36]. First-order interference, although very interesting, is not desirable here and there should not be any first-order interference the purpose of Bell-state preparation.
[34] Branning *et al.*'s scheme uses a $\lambda/2$ plate and a polarizing beam splitter. This setup is essentially equivalent to the scheme with polarizers set at 45°. As pointed out in Ref. [27], Branning *et al.* do not claim Bell-state preparation and therefore there is no need for varying the angles of the analyzers. We are, however, focused on the Bell state preparation. Therefore, it is necessary that angles of the analyzers can be varied arbitrarily.
[35] X.Y. Zou, L.J. Wang, and L. Mandel, Phys. Rev. Lett. **67**, 318 (1991); T.J. Herzog, J.G. Rarity, H. Weinfurter, and A. Zeilinger, *ibid.* **72**, 629 (1994); A.V. Burlakov, M.V. Chekhova, D.N. Klyshko, S.P. Kulik, A.N. Penin, Y.H. Shih, and D.V. Strekalov, Phys. Rev. A **56**, 3214 (1997).
[36] Y.-H. Kim, M.V. Chekhova, S.P. Kulik, Y.H. Shih, and M.H. Rubin, Phys. Rev. A **61**, 051803(R) (2000).
[37] Kwiat *et al.* proposed a similar scheme with a cw pumped SPDC for the purpose of a loophole-free test of Bell's inequality, see Ref. [38].
[38] P.G. Kwiat, P.H. Eberhard, A.M. Steinberg, and R.Y. Chiao, Phys. Rev. A **49**, 3209 (1994).
[39] For 3.4-mm type-II phased matched (400/800 nm) BBO crystal, the maximum transverse walk off between the *e* ray and the *o* ray is 250 μm. Compared with 2.5-mm beam diameter, this is not big, but certainly not negligible.
[40] Y.-H. Kim, S.P. Kulik, and Y.H. Shih, Phys. Rev. A **62**, 011802(R) (2000).
[41] Y.-H. Kim, S.P. Kulik, and Y.H. Shih, Phys. Rev. A (to be published).
[42] Y.-H. Kim, M.V. Chekhova, S.P. Kulik, and Y.H. Shih, Phys. Rev. A **60**, R37 (1999).